

Statistical determination of the length dependence of high-order polarization mode dispersion

A. Eyal, Y. Li, W. K. Marshall, and A. Yariv

Department of Applied Physics, California Institute of Technology, Mail Stop 128-95, Pasadena, California 91125

M. Tur

Department of Interdisciplinary Studies, Faculty of Engineering, Tel Aviv University, Tel Aviv 69978, Israel

Received January 10, 2000

We describe a method of characterizing high-order polarization mode dispersion (PMD). Using a new expansion to approximate the Jones matrix of a polarization-dispersive medium, we study the length dependence of high-order PMD to the fourth order. A simple rule for the asymptotic behavior of PMD for short and long fibers is found. It is also shown that, in long fibers (~ 1000 km), at 40 Gbits/s the third- and fourth-order PMD may become comparable to the second-order PMD. © 2000 Optical Society of America

OCIS codes: 060.0060, 060.2400, 060.4510.

Recently the high-order effects of polarization mode dispersion (PMD) have attracted attention as a potential limiting factor in the performance of high-capacity optical systems.¹⁻³ In this Letter we provide, for what is believed to be the first time, a quantitative study of the statistical properties of PMD for orders higher than the second and show that in long optical links, at transmission rates of 40 Gbits/s (and higher), these high-order effects may become significant.

In the absence of polarization-dependent loss or gain the effect of PMD can be conveniently described in terms of the polarization mode dispersion vector (PMDV), Ω . This three-dimensional vector is used to describe the variation of the output state of polarization, $\hat{s}_{\text{out}}(\omega)$, as a function of the optical frequency ω on the Poincaré sphere. The states of polarization, which are parallel and antiparallel to Ω , are the well-known principal states of polarization (PSP's), and their differential group delay is given by the magnitude of Ω . High-order effects of PMD arise from variation of the PSP's and the differential group delay (or equivalently, variation of Ω) with the optical frequency. It has been shown that the effects of second-order PMD can be described in terms of the frequency derivative of the PMD vector, $\Omega_\omega \equiv \Omega'$.^{1,2} The PMDV and its frequency derivative are three-dimensional random processes whose statistical properties are well established.^{1,4,5}

Until now PMD effects and characteristics higher than the second-order have rarely been treated in the literature. In this Letter we use a recently introduced model³ and a Monte Carlo simulation to compare the magnitudes of the effects of different orders of PMD and to study the length dependence of high-order PMD to the fourth order. The model is based on an exponential expansion of the Jones matrix of the transmission medium. The model reproduces the results of the PMDV-based models and provides a simple and systematic way of extending the analysis to an arbitrary order of PMD and in the presence of polarization-dependent loss or gain.

Let $\mathbf{T}(\omega)$ be the frequency-dependent Jones matrix of a linear transmission medium. The exponential

expansion of $\mathbf{T}(\omega)$ near a given optical frequency ω_0 is expressed as³

$$\begin{aligned} \mathbf{T}(\omega_0 + \Delta\omega) = & \mathbf{T}_0 \exp(\Delta\omega \mathbf{N}_1) \exp\left(\frac{1}{2} \Delta\omega^2 \mathbf{N}_2\right) \\ & \times \exp\left(\frac{1}{6} \Delta\omega^3 \mathbf{N}_3\right) \dots, \end{aligned} \quad (1)$$

where $\Delta\omega \ll \omega_0$, $\mathbf{T}_0 \equiv \mathbf{T}(\omega_0)$, and the characteristic matrices \mathbf{N}_k ($k = 1, 2, 3, \dots$) are 2×2 complex matrices, which one can find by successively differentiating Eq. (1) with respect to $\Delta\omega$ and then substituting $\Delta\omega = 0$. The first four terms in the expansion are given by

$$\begin{aligned} \mathbf{N}_1 &= \mathbf{T}_0^{-1} \mathbf{T}'|_{\omega_0}, \\ \mathbf{N}_2 &= \mathbf{T}_0^{-1} \mathbf{T}''|_{\omega_0} - \mathbf{N}_1^2, \\ \mathbf{N}_3 &= \mathbf{T}_0^{-1} \mathbf{T}'''|_{\omega_0} - \mathbf{N}_1^3 - 3\mathbf{N}_1 \mathbf{N}_2, \\ \mathbf{N}_4 &= \mathbf{T}_0^{-1} \mathbf{T}''''|_{\omega_0} - \mathbf{N}_1^4 - 6\mathbf{N}_1^2 \mathbf{N}_2 - 4\mathbf{N}_1 \mathbf{N}_3 - 3\mathbf{N}_2^2. \end{aligned} \quad (2)$$

Here the primes denote differentiation with respect to frequency. It can be seen that as long as $\mathbf{T}(\omega)$ is nonsingular (i.e., the system does not contain an ideal polarizer) and is differentiable M times, \mathbf{N}_k are well defined for $k = 1, 2, 3, \dots, M$. Using the expansion [Eq. (1)], we can represent each order of PMD as a separate optical system with eigenstates $\hat{e}_{k\pm}$ and eigenvalues $\alpha_{k\pm}$.³ We refer to $\hat{e}_{k\pm}$ as the input principal states of polarization of the k th order, and the difference between the imaginary parts of α_{k+} and α_{k-} , $\delta_k \equiv (\alpha_{k+} - \alpha_{k-})$, defines the magnitude of the k th-order PMD. The first-order eigenstates, $\hat{e}_{1\pm}$, are the well-known (input) PSP's of the medium, and $\text{Im}\{\delta_1\}$ is the differential group delay associated with them.⁶ The correspondence between the first-order descriptors of our model and the PMDV can also be formulated with

a general result from representation theory⁷:

$$\Omega_{1,2,3} = \text{Im}\{\text{Tr}(\mathbf{T}_0 \mathbf{N}_1 \mathbf{T}_0^{-1} \sigma_{3,1,2})\}, \quad (3)$$

where $\Omega_{1,2,3}$ are the elements of Ω and σ_i are the Pauli spin matrices. A similar relation between the second characteristic matrix and Ω_ω can be obtained if we note that formally $d(\mathbf{T}_0^{-1})/d\omega_0 = -\mathbf{T}_0^{-1}(d\mathbf{T}_0/d\omega_0)\mathbf{T}_0^{-1}$ and $\mathbf{N}_2 = d\mathbf{N}_1/d\omega_0$. Thus, differentiating Eq. (3) with respect to ω_0 yields

$$\Omega_{\omega 1,2,3} = \text{Im}\{\text{Tr}(\mathbf{T}_0 \mathbf{N}_2 \mathbf{T}_0^{-1} \sigma_{3,1,2})\}. \quad (4)$$

By explicitly expanding the right-hand side of Eq. (4), it is easy to show that $|\Omega_\omega| = \text{Im}\{\delta_2\}$ and that if no polarization-dependent loss is present (in which case \mathbf{T} is unitary and \mathbf{N}_k are skew Hermitian) the Stokes representations of $\mathbf{T}_0 \hat{e}_{2\pm}$ are aligned with Ω_ω . It was shown in Ref. 3 that in studying the effect of second-order PMD it is useful to consider a medium in which the first-order PMD is compensated for. In such a medium the dominant effect of PMD is the differential quadratic phase acquired by the second-order PSP's. This differential phase is given by $1/2 \Delta \omega^2 \text{Im}\{\delta_2\}$ and leads to differential broadening of pulses. Pulses that are aligned with \hat{e}_{2+} or \hat{e}_{2-} will experience maximum or minimum broadening, respectively. An interesting situation occurs near the frequency of zero average chromatic dispersion (where $\alpha_{2+} + \alpha_{2-} = 0$) in the presence of chirp. In this case α_{2-} is negative, and chirped pulses that are aligned with \hat{e}_{2-} are compressed. This phenomenon was first observed by Poole and Giles.⁸ Our model completes their analysis, as it identifies the two polarization states (the second-order PSP's) in which the effect is maximized.

In the absence of polarization-dependent loss the exponential expansion leads to the following picture on the Poincaré sphere: The state of polarization at the output of a polarization-dispersive medium moves on the sphere as the frequency deviates from ω_0 . At each frequency point the transformation of the state of polarization from its original position (at the input of the medium) can be described by successive rotations. The axes of the rotations are defined by the Stokes representations of $\hat{e}_{k\pm}$, and the angles are given by $1/k! \Delta \omega^k \delta_k \equiv \eta_k$. Hence, for a given bandwidth, $\Delta \omega$, one can use η_k to compare the contributions of the different orders of PMD. Alternatively, we can use them to determine the frequency range in which a k -orders description of PMD is valid. In the presence of polarization-dependent loss or gain this geometrical description is no longer valid, but our model requires no modifications. The k th-order PSP's still exist, although they are no longer orthogonal and $\alpha_{k\pm}$ are not purely imaginary, but their imaginary parts still describe the (k th-order) phase dispersion and η_k can still be used. The real parts of $\alpha_{k\pm}$ may contribute to amplitude dispersion that introduces additional distortion, but this effect is not studied here.

We adopt the stochastic model of Ref. 5 to simulate the randomly fluctuating birefringence in both long and short optical communication fibers. Two fiber sets, one with lengths as great as 500 m and the other

with lengths as great as 1000 km, are studied. Fifty separate realizations for each set are used. For each fiber realization the variances of the first four η_k as a function of fiber length are calculated. Typical values are chosen for the birefringence Δn and the birefringence correlation length^{1,5} h . Simulation results, as well as the well-established^{1,4} theoretical length dependence of $(\langle \Omega^2 \rangle)^{1/2}$ and $(\langle \Omega_\omega^2 \rangle)^{1/2}$, are plotted in Figs. 1 and 2. The specific values of Δn and h that are used ($\Delta n = 3 \times 10^{-7}$, $h = 30$ in Fig. 1 and $\Delta n = 3 \times 10^{-7}$, $h = 25$ in Fig. 2) bear no special significance but were chosen so that η_k can all be plotted together and will be visually distinguishable. The excellent agreement

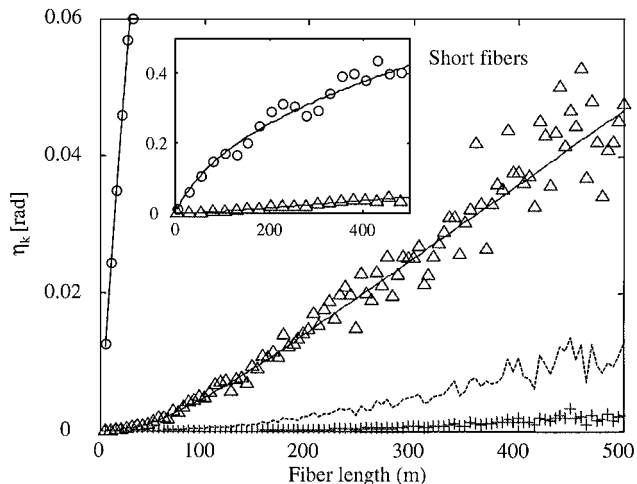


Fig. 1. Length-dependent statistics of the first four orders of PMD for short fibers at the 1-THz bandwidth. The circles, triangles, dashed curve, and plus signs, respectively, represent the simulated first-, second-, third-, and fourth-order PMD, and the solid curves connecting the shapes represent the theoretical predictions for the first- and second-order PMD.

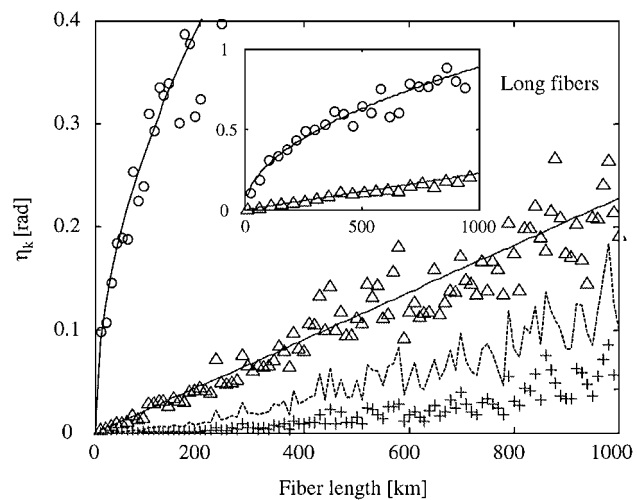


Fig. 2. Length-dependent statistics of the first four orders of PMD for long fibers at 40-GHz bandwidth. The circles, triangles, dashed curve, and plus signs, respectively, represent the simulated first-, second-, third-, and fourth-order PMD, and the solid curves connecting the shapes represent the theoretical prediction for the first- and second-order PMD.

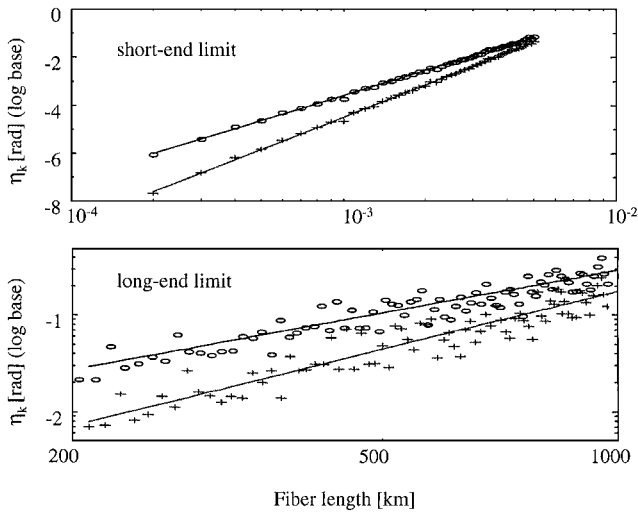


Fig. 3. Top, short-end limit behavior of the third-order (circles) and the fourth-order (plus signs) PMD. Bottom, long-end limit behavior of the third-order (circles) and the fourth-order (plus signs) PMD.

of the calculated statistics of η_1 and η_2 (open circles and triangles, respectively) with the theoretical prediction (solid curves) confirms the validity of our simulation and model. Also shown in Fig. 1 are the length-dependent statistics of the third-order (dashed curves) and fourth-order PMD (plus signs). For the typical values of h and Δn that were chosen, one can see that for a 1000-km-long fiber, the effects of third- and fourth-order PMD become comparable to the second-order PMD at a bandwidth $\Delta f = 40$ GHz. For a 500-m short fiber, on the other hand, the higher-order PMD can be safely neglected even at a bandwidth near 1 THz.

It has been shown in the literature that the first- and second-order PMD assume simple asymptotic behavior. For short fibers the variance of Ω (or η_1) scales linearly with the fiber length L and the variance of Ω_ω (or η_2) scales as $L^{5/2}$; for long fibers, the variances of Ω and Ω_ω scale as $L^{1/2}$ and L^1 , respectively. We have found that similar asymptotic behavior also exists for higher-order PMD effects. In Fig. 3 we show the asymptotic behavior for third- and fourth-order PMD (i.e., η_3 and η_4). According to our least-squares numerical fit, $(\langle\eta_3^2\rangle)^{1/2} \propto L^{3.47}$ and $(\langle\eta_4^2\rangle)^{1/2} \propto L^{4.46}$ in the short-end

limit, and $(\langle\eta_3^2\rangle)^{1/2} \propto L^{1.51}$ and $(\langle\eta_4^2\rangle)^{1/2} \propto L^{2.02}$ in the long-end limit. This strong evidence of tendency leads us to the following proposition: The variance of the k th-order PMD, η_k for $k \geq 2$, scales as $L^{k+1/2}$ in the short-fiber limit and scales as $L^{k/2}$ in the long-fiber limit.

Note that the data spread in the long-fiber limit is much greater than that in short-fiber limit. This is because the long length limit falls in the complete-randomness region, so the relative spread of data is proportional to $1/\sqrt{N}$, where N is the number of realizations. In the short-limit case, however, as we are dealing with lengths $< h$, the resulting data are correlated and show a smaller degree of randomness.

In conclusion, the behavior of higher-order PMD, especially in the long-fiber limit, has important implications for future high-bit-rate optical transmission systems. The exponential expansion approach permits a quantitative comparison of the effects of different orders of PMD. A numerical study of the length dependence of high-order PMD statistically yields a simple rule for the asymptotic behavior of high-order PMD in short and long fibers. This study also shows that in long fibers (~ 1000 km) the third- and fourth-order PMD may become comparable to the second-order PMD at 40 Gbits/s.

The financial support of the U.S. Office of Naval Research and the U.S. Air Force Office of Scientific Research is gratefully acknowledged. A. Eyal's e-mail address is avishay@its.caltech.edu.

References

1. P. Ciprut, B. Gisin, N. Gisin, R. Passy, J. P. Von der Weid, F. Prieto, and C. W. Zimmer, *J. Lightwave Technol.* **16**, 757 (1998).
2. G. J. Foschini, R. M. Jopson, L. E. Nelson, and H. Kogelnik, *J. Lightwave Technol.* **17**, 1560 (1999).
3. A. Eyal, W. K. Marshall, M. Tur, and A. Yariv, *Electron. Lett.* **35**, 1658 (1999).
4. G. J. Foschini and C. D. Poole, *J. Lightwave Technol.* **9**, 1439 (1991).
5. P. K. A. Wai and C. R. Menyuk, *J. Lightwave Technol.* **14**, 148 (1996).
6. B. L. Heffner, *IEEE Photon. Technol. Lett.* **4**, 1066 (1992).
7. N. J. Frigo, *IEEE J. Quantum Electron.* **QE-22**, 2131 (1986).
8. C. D. Poole and C. R. Giles, *Opt. Lett.* **13**, 155 (1988).